

DOI: 10.21802/artm.2025.3.35.71  
UDC 617-002.3:616-001.4:576.3:57.084.1:620.3**CYTOLOGICAL CHARACTERISTICS OF EXPERIMENTAL CHRONIC PURULENT WOUNDS TREATED WITH GRAPHENE OXIDE**

N.M. Ryziuk, O.V. Pyptiuk

*Ivano-Frankivsk National Medical University, Department of Surgical Diseases, Ivano-Frankivsk, Ukraine*  
ORCID ID: 0000-0003-0147-645X, Scopus ID: 7801580852, e-mail: opyptyuk@ifnmu.edu.ua  
ORCID ID: 0000-0003-0364-666X, e-mail: nryziuk@ifnmu.edu.ua

**Abstract.** Chronic purulent wounds remain a serious medical problem due to growing antibiotic resistance of pathogenic microorganisms, requiring new effective therapeutic approaches using nanomaterials. Graphene oxide, as a single-layer functionalized carbon material, exhibits unique antibacterial and regenerative properties due to its large specific surface area of up to 2630 m<sup>2</sup>/g, mechanical strength, and ability to generate reactive oxygen species causing direct physical damage to bacterial cell walls. The mechanism includes membrane integrity disruption through electrostatic interactions, oxidative stress generation, and physical perforation by sharp graphene edges. Unlike conventional antibiotics, resistance to graphene oxide develops extremely slowly, making it attractive for treating multidrug-resistant infections. An experimental study was conducted on 84 laboratory Wistar rats using standardized chronic purulent wound model infected with clinical strains of *Staphylococcus aureus* (ATCC25923), *Escherichia coli* (ATCC25922), and *Pseudomonas aeruginosa* (ATCC27853) at 5×10<sup>9</sup> CFU/ml each. Animals were randomly divided into seven groups of 12: control group receiving sterile saline solution, and six experimental groups using different carriers (ointment mesh, hydrogel dressing, polyurethane sponge) with and without graphene oxide at 0.5 mg/ml concentration. Graphene oxide was characterized by purity >95 %, monolayer thickness 0.7-1.2nm, lateral size 0.5-5µm, C/O ratio 2.1. Wounds were created using 9mm biopsy punch with silicone ring splinting to ensure chronicity. Cytological analysis of impression smears using Pokrovskaya-Makarova method modified by Steinberg was performed on days 3, 6, and 9. Morphometric counting in 10 fields determined cell types, neutrophil destructive changes, macrophage phagocytic activity, and regenerative-degenerative index (RDI). Statistical analysis used one-way ANOVA with Bonferroni correction. Results showed significant healing acceleration in all graphene oxide groups compared to carriers without graphene oxide and saline control. Day 3 demonstrated faster neutrophil infiltration reduction and early macrophage activation with completed phagocytosis signs. Day 6 showed accelerated transition from degenerative-inflammatory to regenerative-inflammatory cytogram types. Day 9 revealed RDI in graphene oxide groups was 4-7 times higher than saline control and 2-3 times higher than corresponding carriers (p<0.001). Clear therapeutic hierarchy emerged: graphene oxide carriers > carriers alone > saline control. Most effective treatments were hydrogel dressing and ointment mesh with graphene oxide, providing optimal moisture balance and prolonged active component release, achieving type V cytograms (regenerative-inflammatory) on day 9. These showed highest macrophage activity, earliest fibroblast formation, and most pronounced angiogenesis. Even carriers without graphene oxide demonstrated 2-3 times higher RDI than natural healing, confirming therapeutic value of proper wound environment management. Results confirm clinical application prospects of graphene oxide for treating chronic purulent wounds with resistant microflora, demonstrating superior outcomes compared to natural healing and significant improvements over carrier-based treatments alone.

**Keywords:** graphene oxide, cytology, purulent wounds, wound healing, neutrophil leukocytes, macrophages, fibroblasts, light microscopy.

**Introduction.** The problem of treating purulent wounds remains one of the most relevant in modern surgery. According to the world health organization, chronic wounds affect 1-2 % of the population in developed countries, and the cost of their treatment accounts for 2-4 % of the total healthcare budget [1, 2]. Purulent-inflammatory diseases of skin and soft tissues occupy a leading place in the structure of nosocomial infections and complications, with mortality reaching 15-25 % in cases of sepsis development [3].

The relevance of the problem increases due to the development of resistance of many microorganism strains to antibiotics and antiseptics. According to the European Centre for Disease Prevention and Control, methicillin resistance among *Staphylococcus aureus* strains is 25-50 % in different European countries [4]. Antibiotic resistance sharply reduces the effectiveness of traditional treatment methods, requires constant updating of the arsenal of medical drugs and the use of complex treatment methods [5].

One of the most promising directions is the use of nanomaterials in medicine. Graphene oxide (GO) is a single-layer sheet of carbon atoms functionalized with oxygen-containing groups (hydroxyl, epoxide, carboxyl, and carbonyl), which gives it unique physicochemical properties. Due to its large specific surface area (up to 2630 m<sup>2</sup>/g), high mechanical strength and biocompatibility, GO exhibits pronounced antibacterial properties against a wide spectrum of microorganisms [6 - 8].

The mechanism of antibacterial action of graphene oxide includes direct physical damage to bacterial cell walls by sharp edges of graphene sheets, oxidative stress through generation of reactive oxygen species, membrane integrity disruption through electrostatic interaction and phospholipid wrapping. Unlike antibiotics, resistance to graphene oxide develops extremely slowly or does not develop at all, making it an attractive alternative to traditional antimicrobial agents [9, 10].

An important condition for improving treatment effectiveness is objective evaluation of the cellular composition of wound exudate, which reflects the sequential stages of healing. Cytological examination allows determining the phase of the wound process, effectiveness of therapeutic measures, and predicting healing times.

**The aim of the study.** To conduct a comparative cytological study of the effectiveness of treating experimental chronic purulent wounds using dressings with graphene oxide compared to corresponding carriers without graphene and traditional treatment methods.

**Materials and methods.** The study used graphene oxide manufactured in the laboratory of colloidal chemistry and high molecular weight compounds chemistry of vasylyshyn precarpathian national university. Material characteristics included purity greater than 95 %, monolayer thickness 0.7-1.2 nm, lateral size 0.5-5  $\mu\text{m}$ , c/o ratio = 2.1. Graphene oxide suspension was prepared in sterile physiological solution at a concentration of 0.5 mg/ml, with ultrasonic treatment for 30 minutes to ensure homogeneity.

The study was conducted on 84 laboratory white Wistar rats (males) with body weight  $180 \pm 20$  g, kept in vivarium conditions in accordance with bioethics requirements. The study was conducted in compliance with the "European Convention for the Protection of Vertebrate Animals Used for Experimental and Other Scientific Purposes" (Strasbourg, 2005) and "General Ethical Principles of Animal Experiments."

Animals were randomly divided into seven groups of 12 animals each. The first group (control) received treatment with sterile 0.9 % saline solution applied twice daily to maintain wound moisture and serve as a neutral control. The second group was treated with ointment mesh without graphene oxide, the third group with ointment mesh containing graphene oxide (0.02 g suspension). The fourth group used hydrogel dressing without graphene oxide, the fifth group used hydrogel dressing with graphene oxide (0.02 g suspension). The sixth group was treated with polyurethane sponge without graphene oxide, and the seventh group with polyurethane sponge containing graphene oxide (0.02 g suspension).

A combined methodology was used to create chronic purulent wounds. Under general anesthesia (ketamine 75 mg/kg + xylazine 10 mg/kg intraperitoneally), two wounds, each with a diameter of 9 mm, were created on the dorsal surface of each animal using a biopsy punch. The skin was excised down to the level of the superficial fascia. To induce purulent infection, a mixture of clinical microbial strains was used: *Staphylococcus aureus* (ATCC 25923), *Escherichia coli* (ATCC 25922), and *Pseudomonas aeruginosa* (ATCC 27853), each at a concentration of  $5 \times 10^9$  CFU/ml. To create conditions for the chronicity of the wound healing process, the wound edges were stabilized with silicone rings to prevent contraction. To induce infection, a defined amount of standardized bacterial suspension (e.g., *Staphylococcus aureus* at a concentration of  $10^8$  CFU/ml) was applied directly to the wound bed using a micropipette or injection syringe. Additional inoculations of the pathogen were repeated as needed on days 3 and 6 to maintain chronicity. The wound was covered with sterile gauze and the dressing was secured.

Cytological examination was performed according to the standardized method of M.P. Pokrovskaya and

M.S. Makarov as modified by D.M. Steinberg. Impression smears were prepared by applying glass slides to the wound surface after removing excess exudate with sterile gauze.

Smears were air-dried, fixed in methyl alcohol for 5 minutes, and stained using the Romanovsky-Giemsa method. Cytological analysis was performed under a light-optical microscope MBR-1 "LOMO" at  $\times 40$  objective magnification (total magnification  $\times 400$ ).

Morphometric cell counting was performed in 10 fields of view (at least 200 cells) with determination of absolute number of different cell types per field of view, percentage of neutrophils with signs of destruction (karyopyknosis, karyorrhexis, karyolysis), percentage of macrophages with signs of phagocytosis, presence and intensity of microbial contamination on a 4-point scale.

The regenerative-degenerative index (RDI) was determined using the formula:  $RDI = NFN/DFN$ , where NFN - number of neutrophils without signs of destruction, DFN - number of neutrophils with signs of destruction per field of view. Cytogram types were classified according to Steinberg. The first type was characterized as necrotic, second type - degenerative-inflammatory, third type - inflammatory, fourth type - inflammatory-regenerative, fifth type - regenerative-inflammatory, sixth type - regenerative.

Statistical processing of results was performed using Statistica 13.0 software. Normality of distribution was checked with the Shapiro-Wilk test. One-way analysis of variance (ANOVA) with post-hoc Tukey test was used for group comparisons. Results are presented as  $M \pm SE$ . Differences were considered statistically significant at  $p < 0.05$ . Multiple comparison correction was performed using the Bonferroni method.

**Research results and their discussion.** On day 3, active inflammatory processes with predominant neutrophil infiltration were observed in all study groups. In the control group receiving sterile saline solution, type I-II cytograms (necrotic to degenerative-inflammatory) were determined, with the vast majority of cells represented by neutrophils showing pronounced destructive changes, virtual absence of macrophages, and abundant microbial flora. The control group demonstrated the slowest healing dynamics, with persistent high levels of neutrophil infiltration and minimal tissue repair activity, representing the natural course of chronic purulent wound healing without active therapeutic intervention.

In groups with carriers without graphene oxide, similar changes were observed: large numbers of neutrophils, isolated macrophages, and presence of microbial flora. In the sponge group without graphene, the vast majority of cells were represented by neutrophils, macrophages were virtually absent, and large amounts of microbial flora were observed; type II cytograms (degenerative-inflammatory) were determined. The mesh group without graphene was characterized by large numbers of neutrophils, isolated macrophages, and large amounts of microbial flora and detritus; type II cytograms (inflammatory) were also determined. The best indicators among carriers without graphene oxide were demonstrated by hydrogel without graphene—type III cytograms (inflammatory) with fewer destructive forms of neutrophils, large numbers of neutrophils, numerous macrophages, isolated lymphocytes, and virtually absent microbial flora (Fig. 1).

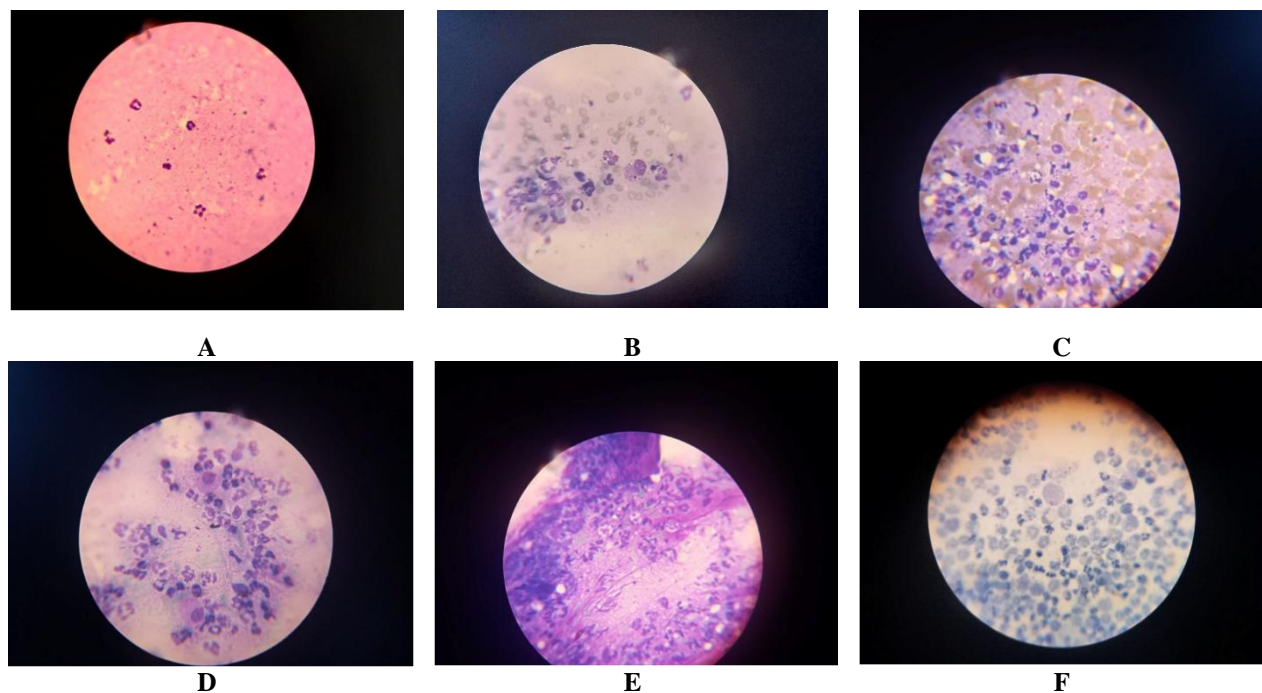


**Fig. 1. Impression smears of experimental wounds on day 3: a — sponge without graphene oxide, b — sponge with graphene oxide, c — mesh without graphene oxide, d — mesh with graphene oxide, e — hydrogel without graphene oxide, f — hydrogel with graphene oxide. Romanovsky-giemsa staining,  $\times 400$**

The addition of graphene oxide to all types of carriers led to improvement of the cytological picture. In the "sponge + graphene oxide" group, neutrophils and macrophages with phagocytosed inclusions were observed (indicating active wound cleansing), along with lymphocytes, detritus, and erythrocytes. A transitional type II-III cytogram (degenerative-inflammatory to inflammatory) was determined (Fig. 1).

In the "mesh + graphene oxide" group, the number of neutrophils was smaller compared to the mesh without graphene oxide, the number of phagocytic macrophages increased, and microbial flora was present in significantly smaller amounts. A transitional type II-III cytogram (degenerative-inflammatory to inflammatory) was determined.

The best results on day 3 were shown by the "hydrogel + graphene oxide" group: the number of neutrophils decreased, macrophages with phagocytic inclusions were observed, and microflora was virtually absent. Type III cytograms (inflammatory) were determined (Fig. 1).

On day 6, all groups showed a statistically significant decrease in leukocyte count compared to day 3, indicating decreased intensity of the inflammatory process. The control group with saline solution showed limited improvement with persistent type II cytograms (degenerative-inflammatory), with neutrophil counts remaining significantly higher compared to all carrier groups, minimal macrophage activation, and continued presence of abundant microbial flora.

In groups with carriers without graphene, moderate improvements were observed. In the "mesh without

graphene" group, neutrophils, macrophages, early fibroblast formation, and isolated endotheliocytes were observed, indicating active repair. Type III-IV cytograms (inflammatory to inflammatory-regenerative) were determined. In the "sponge without graphene" group, neutrophils predominated, with isolated macrophages and small numbers of erythrocytes present; type III-IV cytograms were also determined. The "hydrogel without graphene" group was characterized by the presence of neutrophils, macrophages, and the appearance of fibroblasts; type III-IV cytograms (inflammatory to inflammatory-regenerative) were determined (Fig. 2).

Groups with graphene oxide showed significantly better results. In the "mesh + graphene oxide" group, insignificant number of neutrophils was observed, indicating transition from inflammatory to proliferative phase, large number of macrophages, fibroblasts, and endotheliocyte formation (angiogenesis). Type IV cytogram (inflammatory-regenerative) was determined.

In the "sponge + graphene oxide" group, neutrophils were present in smaller numbers, indicating transition to the repair stage, with macrophages and early fibroblast formation present. Unlike the sponge without graphene oxide, erythrocytes were not observed. Type IV cytograms (inflammatory-regenerative) were determined.

The "hydrogel + graphene oxide" group was characterized by decreased number of neutrophils, presence of macrophages and fibroblasts. Type IV cytogram (inflammatory-regenerative) was determined.

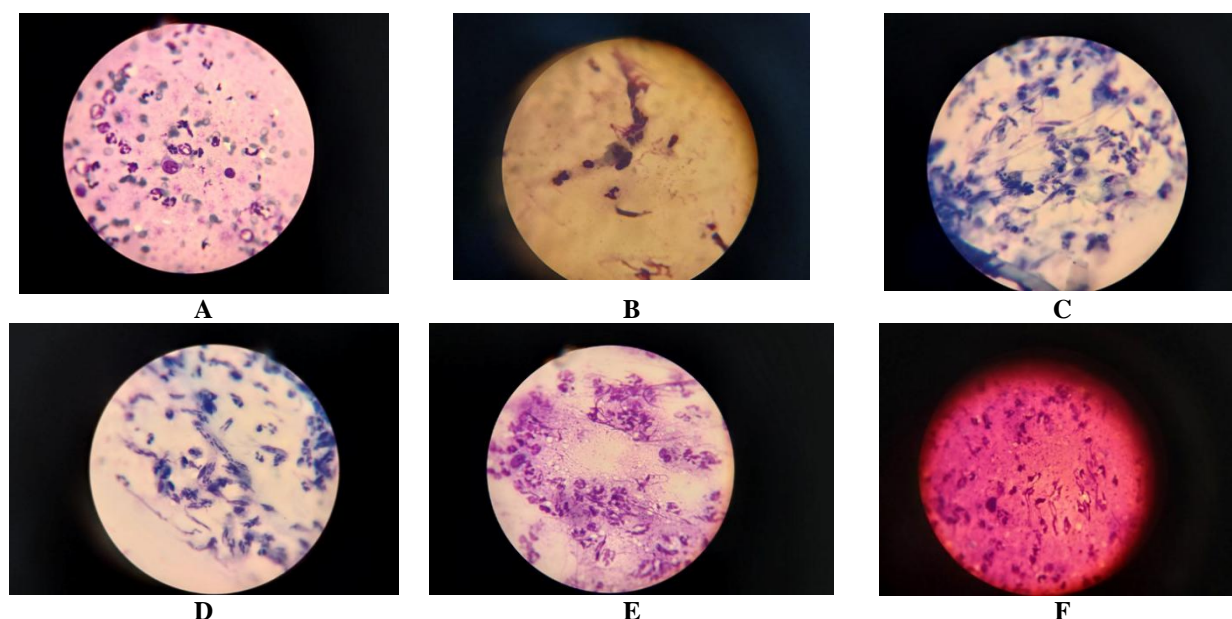


**Fig. 2. Impression smears of experimental wounds on day 6: A — sponge without graphene oxide, B — sponge with graphene oxide, C — mesh without graphene oxide, D — mesh with graphene oxide, E — hydrogel without graphene oxide, F — hydrogel with graphene oxide. Romanovsky-Giemsa staining, ×400**

On day 9 of the experiment, cytological indicators clearly reflected different stages of wound process in the studied groups. The control group with saline solution demonstrated persistent type II-III cytograms (degenerative-inflammatory to inflammatory) with continued high neutrophil infiltration, limited macrophage activity, minimal fibroblast formation, and the slowest overall healing progression, representing the natural healing course without therapeutic intervention.

In groups with carriers without graphene, slower improvement was observed. The "sponge without graphene" group was characterized by significant decrease in

neutrophil number, isolated erythrocytes, presence of macrophages and fibroblasts, type IV cytogram (inflammatory-regenerative) was determined. In the "mesh without graphene" group, neutrophils were practically absent, macrophages and fibroblasts were observed, type IV-V cytogram (inflammatory-regenerative - regenerative-inflammatory) was determined. The "hydrogel without graphene" group demonstrated practical absence of neutrophils, erythrocytes, lymphocytes, macrophages, and isolated fibroblasts, type IV cytogram (inflammatory-regenerative) was determined (Fig. 3).

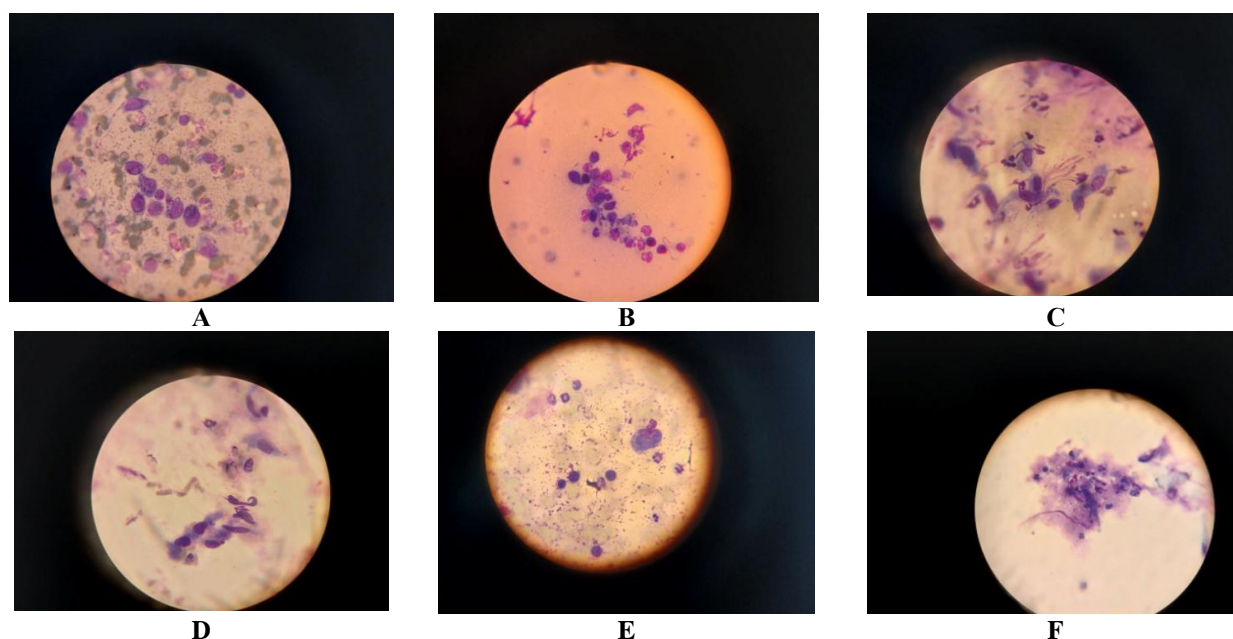


**Fig. 3. Impression smears of experimental wounds on day 9: A — sponge without graphene oxide, B — sponge with graphene oxide, C — mesh without graphene oxide, D — mesh with graphene oxide, E — hydrogel without graphene oxide, F — hydrogel with graphene oxide. Romanovsky-Giemsa staining, ×400**

The best results were shown by groups with graphene oxide. In the "sponge + graphene oxide" group, significant decrease in neutrophil number, predominance of macrophages and fibroblasts were observed. Type IV-V cytogram (inflammatory-regenerative - regenerative-inflammatory) was determined.

In the "mesh + graphene oxide" group, small numbers of neutrophils, macrophages, and increased numbers of fibroblasts compared to the mesh without graphene oxide were noted, along with the presence of fibers. Type V cytograms (regenerative-inflammatory) were determined.

The best results were shown by the "hydrogel + graphene oxide" group: neutrophils were practically not observed, isolated lymphocytes, macrophages, fibroblasts, and fibers were present. Type V cytogram (regenerative-inflammatory) was determined (Fig. 3).

Statistical analysis showed significant differences between all treatment groups at all stages of the study (Table 1).

The most pronounced differences were observed on day 9, when the RDI in groups with graphene was 4-7 times higher compared to the saline control group, 2-3 times higher compared to carriers without graphene oxide. Importantly, even carriers without graphene oxide showed 2-3 times higher RDI compared to the saline control, demonstrating the therapeutic value of the carrier-based approach itself. The hierarchy of effectiveness was clearly established: graphene oxide-containing carriers > carriers without graphene oxide > saline control.

The obtained results demonstrate pronounced reparative activity of graphene oxide in treating experimental chronic purulent wounds compared to both carriers without graphene oxide and saline control treatment. The saline control group, representing the natural healing process without therapeutic intervention, showed the slowest healing dynamics with persistent inflammatory phase, minimal tissue repair activity, and high microbial contamination throughout the study period.

The mechanism of GO action includes several components: direct antibacterial action through physical damage to bacterial cell walls, generation of reactive oxygen species, stimulation of macrophage activity, and acceleration of neoangiogenesis. The antibacterial effectiveness of graphene oxide is confirmed by significant reduction of microbial contamination in all experimental groups as early as day 3, with dramatic improvements compared to the natural healing process observed in the saline control group.

Accelerated transition from inflammatory to proliferative phase of healing in groups with graphene oxide is confirmed by early formation of fibroblasts (from day 6) and endotheliocytes, indicating active angiogenesis. This may be related to GO's modulating influence on

expression of growth factors and cytokines that regulate repair processes.

Among the studied carriers, the best results were shown by hydrogel dressing and ointment mesh with graphene oxide. Hydrogel provides optimal wound surface moisture and prolonged release of active substances, while ointment base promotes better contact with wound tissues. Importantly, even carriers without graphene oxide showed dramatically better healing outcomes than the saline control, demonstrating that proper wound environment management through carrier-based approaches provides substantial therapeutic benefits beyond simple moisture maintenance.

**Conclusions.** The addition of graphene oxide to all studied carriers (ointment mesh, hydrogel dressing, polyurethane sponge) leads to significant acceleration of healing in experimental chronic purulent wounds compared to corresponding carriers without graphene oxide and natural healing process observed with saline control treatment.

The most effective treatments were hydrogel dressing and ointment mesh with graphene oxide, which provided the fastest transition to type V cytograms (regenerative-inflammatory) on day 9 of the experiment, demonstrating superior outcomes compared to all control treatments.

A clear therapeutic hierarchy was established: graphene oxide-containing carriers showed 4-7 times higher regenerative-degenerative index compared to saline control, while carriers without graphene oxide demonstrated 2-3 times higher index than natural healing, confirming both the specific benefits of graphene oxide and the general therapeutic value of carrier-based wound management.

Cytological criteria for treatment effectiveness include: significant decrease in neutrophil numbers and their destructive forms, increased numbers of macrophages with signs of phagocytosis, early formation of fibroblasts and endotheliocytes, and increased regenerative-degenerative index. These criteria demonstrated clear dose-response relationship across the treatment spectrum from natural healing through carrier-based treatments to graphene oxide-enhanced therapy.

The application of graphene oxide represents a promising direction for clinical implementation in treating chronic purulent wounds, demonstrating dramatic advantages over natural healing processes and significant improvements over carrier-based treatments alone, but requires further safety studies and optimization of concentrations for clinical translation.

**Conflict of interest:** absent.

Table 1

Dynamics of Main Cytological Indicators (M ± SE)

Indicators	Day 3				Day 6				Day 9			
	Control (Saline)	Carrier without GO	Carrier + GO	p-value*	Control (Saline)	Carrier without GO	Carrier + GO	p-value*	Control (Saline)	Carrier without GO	Carrier + GO	p-value*
<b>OINTMENT MESH</b>												
Neutrophils per field	58±5	47±4	39±3	<0.001	45±4	35±3	22±2	<0.001	35±3	18±2	8±1	<0.001
Macrophages per field	1±0	3±1	6±1	<0.001	3±1	8±1	14±2	<0.001	5±1	12±2	18±2	<0.001
Fibroblasts per field	0	0	0	-	0±0	2±1	5±1	<0.001	2±1	6±1	12±2	<0.001
Endotheliocytes per field	0	0	0	-	0	1±0	3±1	<0.001	0±0	2±1	5±1	<0.001
RDI	0.08±0.02	0.19±0.03	0.28±0.04	<0.001	0.25±0.04	0.65±0.08	1.12±0.15	<0.001	0.95±0.12	2.15±0.25	4.85±0.45	<0.001
<b>HYDROGEL</b>												
Neutrophils per field	55±4	41±3	32±3	<0.001	42±3	28±2	18±2	<0.001	32±3	14±2	6±1	<0.001
Macrophages per field	1±0	5±1	8±1	<0.001	4±1	10±1	16±2	<0.001	6±1	15±2	22±3	<0.001
Fibroblasts per field	0	0	0	-	1±0	3±1	6±1	<0.001	3±1	8±1	15±2	<0.001
Endotheliocytes per field	0	0	0	-	0	0	2±1	<0.01	0±0	1±0	4±1	<0.001
RDI	0.09±0.02	0.22±0.04	0.35±0.05	<0.001	0.32±0.05	0.78±0.10	1.35±0.18	<0.001	1.15±0.15	2.45±0.28	5.25±0.52	<0.001
<b>POLYURETHANE SPONGE</b>												
Neutrophils per field	62±5	52±4	43±3	<0.001	48±4	38±3	26±2	<0.001	38±3	22±2	12±1	<0.001
Macrophages per field	1±0	2±1	5±1	<0.01	2±1	6±1	11±2	<0.001	4±1	10±2	16±2	<0.001
Fibroblasts per field	0	0	0	-	0±0	1±0	3±1	<0.001	1±0	5±1	9±1	<0.001
Endotheliocytes per field	0	0	0	-	0	0	1±0	<0.05	0±0	1±0	3±1	<0.01
RDI	0.06±0.01	0.16±0.03	0.24±0.04	<0.001	0.22±0.04	0.58±0.07	0.95±0.12	<0.001	0.75±0.10	1.85±0.22	3.45±0.35	<0.001

Note: \*p-value for comparison between all three groups using one-way ANOVA

**References:**

1. Hassen A, Moawed EA, Bahy R, El Basaty AB, El-Sayed S, Ali AI, et al. Synergistic effects of thermally reduced graphene oxide/zinc oxide composite material on microbial infection for wound healing applications. *Sci Rep*. 2024; 14(1):22942.
2. Soliman M, Sadek AA, Abdelhamid HN, Hussein K. Graphene oxide-cellulose nanocomposite accelerates skin wound healing. *Res Vet Sci*. 2021; 137:262-73.
3. Di Lodovico S, Diban F, Di Fermo P, Petrini M, Fontana A, Di Giulio M, et al. Antimicrobial combined action of graphene oxide and light emitting diodes for chronic wound management. *Int J Mol Sci*. 2022; 23(13):6942.
4. Fadhil WA, Jabbar II, Ali EH, Sulaiman GM, Khan RA, Mohammed HA. Freshly prepared graphene oxide nanoparticles' wound-healing potential and antibacterial activity specifically against staphylococcus aureus. *Plasmonics*. 2025; 20(2):763-73.
5. Luz EPCG, da Silva TF, Marques LSM, Andrade A, Lorevice MVV, Andrade FK, et al. Bacteria-derived cellulose membranes modified with graphene oxide-silver nanoparticles for accelerating wound healing. *ACS Appl Bio Mater*. 2024; 7(8):5530-40.
6. Mohammadi A, Kerdabadi ZG, Najafabadi SAA, Pourali A, Nejaddehbash F, Azarbarz N, et al. A high-efficient antibacterial and biocompatible polyurethane film with Ag@rGO nanostructures prepared by microwave-assisted method: Physicochemical and dermal wound healing evaluation. *Heliyon*. 2023; 9(11):e22142.
7. Li Y, Wang J, Yang Y, Shi J, Zhang H, Yao X, et al. A rose bengal/graphene oxide/PVA hybrid hydrogel with enhanced mechanical properties and light-triggered antibacterial activity for wound treatment. *Mater Sci Eng C*. 2021; 118:111447.
8. Chen J, Wang X, Han H. A new function of graphene oxide emerges: inactivating phytopathogenic bacterium *Xanthomonas oryzae* pv. *Oryzae*. *J Nanopart Res*. 2022; 24(3):48.
9. Augustine R, Hasan A, Patan NK, Dalvi YB, Varghese R, Antony A, et al. Cerium oxide nanoparticle incorporated electrospun poly(3-hydroxybutyrate-co-3-hydroxyvalerate) membranes for diabetic wound healing applications. *ACS Biomater Sci Eng*. 2020; 6(1):58-70.
10. Akhavan O, Ghaderi E. Toxicity of graphene and graphene oxide nanowalls against bacteria. *ACS Nano*. 2010; 4(10):5731-6.

УДК 617-002.3:616-001.4:576.3:57.084.1:620.3

**ЦИТОЛОГІЧНА ХАРАКТЕРИСТИКА  
ЕКСПЕРИМЕНТАЛЬНИХ ХРОНІЧНИХ  
ГНІЙНИХ РАН З ВИКОРИСТАННЯМ ОКСИДУ  
ГРАФЕНУ ПІД ЧАС ЛІКУВАННЯ**

Н.М. Ризюк, О.В. Пиптюк

Івано-Франківський національний медичний університет, кафедра хірургічних хвороб,  
м. Івано-Франківськ, Україна  
ORCID ID: 0000-0003-0147-645X,  
Scopus ID: 7801580852,  
e-mail: opruytyuk@ifnmu.edu.ua  
ORCID ID: 0000-0003-0364-666X,  
e-mail: nryziuk@ifnmu.edu.ua

**Резюме.** Хронічні гнійні рани залишаються серйозною медичною проблемою через зростання антибіотикорезистентності патогенних мікроорганізмів, що вимагає пошуку нових ефективних терапевтичних підходів із використанням наноматеріалів. Оксид графену як одношаровий функціоналізований вуглецевий матеріал виявляє унікальні антибактеріальні й регенеративні властивості завдяки великій питомій поверхні до 2630 м<sup>2</sup>/г, механічній міцності та здатності генерувати активні форми кисню, що спричиняють пряме фізичне пошкодження бактеріальних клітинних стінок. Експериментальне дослідження проведено на 84 лабораторних щурах лінії Wistar із використанням моделі хронічних гнійних ран, інфікованих клінічними штамми *Staphylococcus aureus*, *Escherichia coli* та *Pseudomonas aeruginosa* концентрацією 5×10<sup>9</sup> КУО/мл кожного. Тварини були розподілені на сім груп із використанням різних носіїв: мазевої сітки, гідрогелевої пов'язки і поліуретанової губки з оксидом графену та без нього в концентрації 0,5 мг/мл, а також контрольної групи, що отримувала традиційне антисептичне лікування. Цитологічний аналіз мазків-відбитків за методикою Покровської-Макарова в модифікації Штейнберга на 3-тю, 6-ту та 9-ту добу показав значне прискорення загоєння в усіх групах з оксидом графену порівняно з контрольними. Спостерігалось швидше зменшення нейтрофільної інфільтрації разом із раннім активуванням макрофагів з ознаками завершеного фагоцитозу та прискореним переходом від дегенеративно-запального до регенеративно-запального типів цитограм. Це підтверджувалося зростанням регенеративно-дегенеративного індексу в 2-3 рази. Найефективнішими виявилися гідрогелева пов'язка й мазева сітка з оксидом графену, які забезпечували оптимальний вологий баланс і пролонговане вивільнення активних компонентів, досягаючи V типу цитограми на 9-ту добу експерименту. Результати підтверджують перспективність клінічного застосування оксиду графену для лікування хронічних гнійних ран із резистентною мікрофлорою.

**Ключові слова:** оксид графену, цитологія, гнійні рани, загоєння ран, нейтрофільні лейкоцити, макрофаги, фібробласти, світлова мікроскопія.

**Конфлікт інтересів:** відсутній.

Стаття надійшла в редакцію 08.08.2025 р.  
Стаття прийнята до друку 23.08.2025 р.